Phosphorescence-Fluorescence ratio imaging for monitoring the oxygen status during photodynamic therapy

H. J. C. M. Sterenborg, J.W. de Wolf, M. Koning, B Kruijt, A. van den Heuvel, D. J. Robinson

Photodynamic Therapy and Optical Spectroscopy Research Programme, Department of Radiation Oncology, Erasmus University Medical Center, Rotterdam, The Netherlands
h.j.c.m.sterenborg@erasmusmc.nl d.robinson@erasmusmc.nl

http://www.erasmusmc.nl/radiotherapie/4/3/photodynamic_therapy.htm

Abstract: The effectiveness of photodynamic therapy is strongly dependent on the availabilty of oxygen. In the present paper we show that the ratio between photosensitiser phosphorescence and fluorescence is a parameter that can be used to monitor the competition between singlet oxygen production and other processes quenching the photosensitiser triplet state. We present a theoretical basis for the validity of this approach and a series of in vitro imaging experiments.

OCIS codes: (170.5180) Photodynamic therapy; (120.3890) Medical optics instrumentation; (170.3880) Medical and biological imaging

References and links

1. W.M. Star, "Light dosimetry in vivo," Phys. Med. Biol. **42,** 763-87 (1997).
2. B.C. Wilson, M.S. Patterson, L. Lilge "Implicit and Explicit Dosimetry in Photodynamic Therapy: A New Paradigm," Lasers Med. Sci. **12,** 182-99 (1997)
3. D.J. Robinson, H.S. de Bruijn, N. van der Veen, M.R. Stringer, S.B. Brown, W.M Star. "Fluorescence photobleaching of ALA-induced protoporphyrin IX during photodynamic therapy of normal hairless mouse skin: the effect of light dose and irradiance and the resulting biological effect," Photochem. Photobiol. **67,** 140-9 (1998)
4. D.J. Robinson, H.S. de Bruijn, W.J. de Wolf, H.J.C.M. Sterenborg, W.M. Star. "Topical 5-aminolevulinic acid-photodynamic therapy of hairless mouse skin using two-fold illumination schemes: PpIX fluorescence kinetics, photobleaching and biological effect," Photochem. Photobiol. **72,**794- 802 (2000)
5. I.A. Boere, D.J. Robinson, H.S. de Bruijn, J. van den Boogert, H.W. Tilanus, H.J.C.M. Sterenborg, R.W. de Bruin. "Monitoring in situ dosimetry and protoporphyrin IX fluorescence photobleaching in the normal rat esophagus during 5-aminolevulinic acid photodynamic therapy," Photochem. Photobiol. **78,** 271-7 (2003)
6. J.S. Dysart, M.S. Patterson, T.J. Farrell, G. Singh . "Relationship between mTHPC fluorescence photobleaching and cell viability during in vitro photodynamic treatment of DP16 cells" Photochem. Photobiol. **75,** 289-95 (2002)
7. J.C. Finlay, S. Mitra , T.H. Foster. "In vivo mTHPC photobleaching in normal rat skin exhibits unique irradiance-dependent features," Photochem. Photobiol. **75,** 282-8 (2002)
8. L. Kunz , A.J. MacRobert. "Intracellular photobleaching of 5,10,15,20-tetrakis(m-hydroxyphenyl) chlorin exhibits a complex dependence on oxygen level and fluence rate," Photochem. Photobiol. **75,** 28-35 (2002)
9. V.X. Yang , P.J. Muller, P. Herman , B.C. Wilson . "A multispectral fluorescence imaging system: design and initial clinical tests in intra-operative" Photofrin-photodynamic therapy of brain tumors. Lasers Surg. Med. **32,:** 224-32 (2003)
10. H. Zeng, M. Korbelik, D.I. McLean, C. MacAulay , H. Lui. "Monitoring photoproduct formation and photobleaching by fluorescence spectroscopy has the potential to improve PDT dosimetry with a verteporfin-like photosensitizer," Photochem. Photobiol. **75,** 398-405 (2002)
11. J.G. Parker. "Optical monitoring of singlet oxygen during photodynamic treatment of tumors," IEEE Circ. Devices Mag. 10-21. (1987)
12. M.S. Patterson, S.J. Madsen, B.C. Wilson. "Experimental tests of the feasibility of singlet oxygen luminescence monitoring in vivo during photodynamic therapy," J. Photochem. Photobiol. B. **5,** 69-84 (1990)

#4089 - $15.00 US Received 25 March 2004; revised 9 April 2004; accepted 15 April 2004

13. M.J. Niedre , M.S. Patterson, B.C. Wilson. "Direct near-infrared luminescence detection of singlet oxygen generated by photodynamic therapy in cells in vitro and tissues in vivo," Photochem. Photobiol. **75:** 382-91 (2002)
14. B.W. Pogue, T. Momma , H.C. Wu, T. Hasan "Transient absorption changes in vivo during photodynamic therapy with pulsed-laser light," Br. J. Cancer **80,** 344-351 (1999)
15. H.J.C.M. Sterenborg, M. Janson, M.J.C. van Gemert. "A novel frequency domain technique for measurement of triplet decay times using two diode lasers," Phys.Med. Biol. **44,** 1419-1426 (1999)
16. M.J. Niedre, A.J. Secord, M.S. Patterson, B.C. Wilson. "In vitro tests of the validity of singlet oxygen luminescence measurements as a dose metric in photodynamic therapy," Cancer Res. **63,** 7986-9 (2003)
17. S. Gross, A. Gilead, A. Scherz, M. Neeman, Y. Salomon. "Monitoring photodynamic therapy of solid tumors online by BOLD-contrast MRI," Nat. Med. **9,** 1327-31 (2003)
18. H.J.C.M. Sterenborg, M.J.C. van Gemert. "Photodynamic therapy with pulsed sources; a theoretical analysis," Phys. Med. Biol. **41,** 835-50 (1994)
19. T.H. Foster, R.S. Murant, R.G. Bryant, R.S. Knox, S.L. Gibson, R.Hilf. "Oxygen consumption and diffusion effects in photodynamic therapy," Radiat. Res. **126,** 296-303 (1991)

1. Introduction

In recent years, dosimetry for clinical photodynamic therapy (PDT) has remained focused on the dosimetry of light and administered photosensitiser [1]. While state-of-the-art light dosimetry is critically important for limiting the light dose delivered to vulnerable areas of tissue it has been shown not to be a reliable predictor of therapeutic effect of PDT. This is because the photodynamic efficacy, expressed as the actual singlet oxygen production within the illuminated volume is determined by the local sensitiser concentration, the local fluence rate and the local concentration of ground state oxygen. The incorporation of these parameters is of vital importance for predictable and resproducible PDT. The concept of implicit dosimetry introduced by Wilson *et al*. [2] involves measuring various changing properties of the photosensitiser, such as the photobleaching rate constant, or triplet decay time, to determine the singlet oxygen production during PDT. Several possibilities for obtaining such signals during PDT have been investigated, with varying degrees of success. We have shown that for the photosensitiser aminolevulinic acid (ALA)-induced protoporphyrin (PpIX) the rate of photobleaching and tissue response increase with decreasing fluence rate [3] and the kinetics of photobleaching are influenced by light fractionation [4]. We have also shown that during oesophageal photodynamic therapy with ALA when in situ light dosimetry is used to standardise the fluence rate a wide range of photobleaching rates are observed [5]. Here the rate and extent of PpIX photobleaching is predictive of tissue response. The photobleaching of other photosensitisers has also been investigated. An in-vitro study using m-THPC [6] suggests that fluorescence photobleaching can be used as a predictor of PDT damage, however other investigators have reported more complex kinetics both *in-vivo* [7] and in different cellular compartments [8]. The relationship between mTHPC photobleaching and tissue response *in-vivo* is not yet clear. A system for measuring Photofrin photobleaching has recently been developed for the use in neurosurgery [9]. The photobleaching of Vertoporfin has also been investigated and Zeng *et al.* [10] have formulated a parameter that utilises the ratio of photoproduct to photosensitiser fluorescence to predict the response of tissues to PDT. A number of alternative dose metrics to fluorescence photobleaching have been investigated. Direct singlet oxygen luminescence measurements during PDT [11-13] as well as photosensitiser triplet decay time measurements in the time and frequency domain [14,15] have shown promising results but have all been difficult to reproduce clinically. Niedre *et al.* have recently shown that there is a direct relationship between singlet oxygen luminescence and cell kill in vitro [16]. A new method of monitoring PDT with the photosensitiser Pd-Bacteriopheophorbide (TOOKAD) has recently been reported in which the palladium atom within the porphyrin ring provides MR contrast and allows oxygen partial pressures to be determined using BOLD contrast MRI [17].

What is clear from the work on implicit dosimetry published to date is that the appropriate technique is critically photosensitiser dependent and hence there remains a need

#4089 - $15.00 US Received 25 March 2004; revised 9 April 2004; accepted 15 April 2004

for alternative techniques for implicit dosimetry that can be applied in vivo. Even techniques that would not be practical for clinical use could still be of great value for experimental studies helping us reveal the many unanswered questions on the fundamentals of PDT. In the present paper we present the theoretical basis for the use of photosensitiser phosphorescence as a source of information for implicit dosimetry that is complementary to many of the other methods that have been developed, and an in vitro experiment to demonstrate its feasibility.

2. Materials and methods

2.1 Theoretical background

Similar to that we have described previously [18], but with a term added to account for the phosphorescence, A_{20}, the rate equations governing the population and depopulation of the ground, singlet and triplet states of the photosensitiser are:

$$\begin{aligned}
\frac{\partial[N_0(t)]}{\partial t} &= -[N_0(t)]B_{01}\Phi(t) + [N_1(t)](A_{10}+k_{10}) + [N_2(t)](A_{20}+k_{20}+q[{}^3O_2(t)]) \\
\frac{\partial[N_1(t)]}{\partial t} &= +[N_0(t)]B_{01}\Phi(t) - [N_1(t)](A_{10}+k_{10}+k_{12}) \\
\frac{\partial[N_2(t)]}{\partial t} &= +[N_1(t)]k_{21} - [N_2(t)](A_{20}+k_{20}+q[{}^3O_2(t)])
\end{aligned} \tag{1}$$

where $[N_0(t)]$, $[N_1(t)]$ and $[N_2(t)]$ are the time dependent concentrations of the photosensitiser singlet ground state, the singlet excited state and the triplet ground state, $\Phi(t)$ is the fluence rate, $A_{i,j}$ is the rate constant for the radiatiative and $k_{i,j}$ for the radiationless transition rates from state i to state j, q is the bimolecular quenching rate constant of the triplet state by ground state oxygen and $[{}^3O_2(t)]$ the ground state oxygen concentration. Since we are dealing with relatively slow quasistatic changes in the populations (with respect to the transition rates) we can work with the equilibrium solution to Eq. (1):

$$\begin{aligned}
[N_0] &= N_{00} \\
[N_1] &= \frac{N_{00}B_{01}\Phi}{(A_{10}+k_{10}+k_{12})} \\
[N_2] &= \frac{N_{00}B_{01}\Phi k_{21}}{(A_{20}+k_{20}+q[{}^3O_2])(A_{10}+k_{10}+k_{12})}
\end{aligned} \tag{2}$$

where $[N_0]$, $[N_1]$ and $[N_2]$ stand for the equilibrium concentrations of singlet and triplet excited states and N_{00} stands for the total concentration of photosensitiser molecules. This step has further assumed that the fluence rates are far below saturation levels; i.e., no substantial depletion of the ground state population occurs, i.e., $[N_1]$ and $[N_2] << N_{00}$ [18]. The singlet oxygen production term can now be easily quantified as:

$$\textit{Singlet Oxygen production} = [N_2]q[{}^3O_2] \tag{3}$$

Quenching by oxygen is not the only mechanism of depopulation of the photosensitiser triplet state. Both spontaneous decay (decay rate k_{20}) and phosphorescence (decay rate A_{20}) are in direct competition with singlet oxygen production. We express this by a parameter α:

$$\alpha = \frac{q[{}^3O_2]}{(A_{20}+k_{20}+q[{}^3O_2])} \tag{4}$$

where α goes to zero at low levels of $[{}^3O_2]$. Alfa describes the fraction of the triplet state quenching events that lead to the production of singlet oxygen. Equation (4) clearly illustrates the underlying problem with the response of tissues to PDT: the effectiveness of PDT can be

#4089 - $15.00 US Received 25 March 2004; revised 9 April 2004; accepted 15 April 2004

reasonable at high tissue oxygen levels but goes to zero below a critical oxygen level. From Eq. (2) the steady state fluorescence (F) and phosphorescence (P) can be derived as:

$$F = A_{10}[N_1] = N_{00} B_{01} \Phi \frac{A_{10}}{(A_{10} + k_{10} + k_{12})}$$
$$P = A_{20}[N_2] = N_{00} B_{01} \Phi \frac{A_{20} k_{21}}{(A_{20} + k_{20} + q[{}^3O_2])(A_{10} + k_{10} + k_{12})} \quad (5)$$

The ratio of the 2 yields:

$$\frac{P}{F} = \frac{A_{20}[N_2]}{A_{10}[N_1]} = \frac{A_{20} k_{21}}{A_{10}(A_{20} + k_{20} + q[{}^3O_2])} = \gamma(1-\alpha)$$
$$\text{with } \gamma = \frac{k_{21} A_{20}}{(A_{20} + k_{20}) A_{10}} \quad (6)$$

So, the signal defined by the ratio of phosphorescence and fluorescence is proportional to a constant γ multiplied by 1 minus the relative effectiveness of the treatment.

2.2. Experiments

Sn (IV) mesoporphyrin IX dichloride (SnMP; Frontier Scientific, Carnforth, UK) was dissolved in 1% albumin and excited using 408 nm radiation from an LED light source (Roithner, Vienna, AT). The variation in emission spectrum, acquired using a simple CCD spectrograph (Avantes, Eerbeek, NL.) with pO_2 is shown in Fig. 1. Measurements were performed in a 10-mm pathlength quartz cuvette with a clear solution of 10 µg/l SnMP. Oxygen measurements were performed using a pO_2 sensor needle (Unisense, Aarhus, DK). Emission below 600 nm is independent of pO_2 and represents the fluorescence emission of SnMP. The peak centered on 716 nm is due to SnMP phosphorescence.

An imaging system consisting of a 2-stage peltier cooled slow scan CCD camera (Princeton Intruments Inc Princeton NJ, USA) equipped with a computer controlled filter

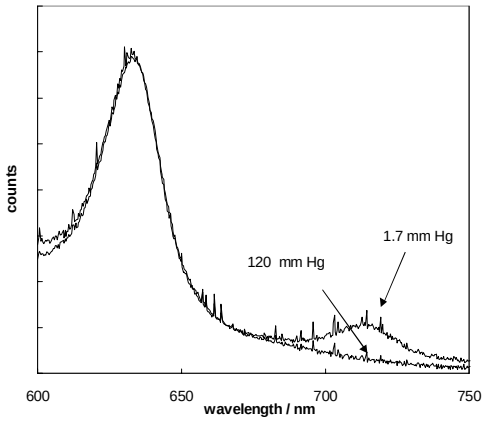

Fig. 1. Emission spectrum of 10 µg Sn-Mesoporphyrin in 1% albumin at different pO_2 levels.

wheel (Fairlight, Rotterdam, NL) and a f2.8/105 mm macro lens was used to acquire fluorescence and phosphorescence images from a quartz cuvette containing 10 µg/l SnMP. Camera, filter wheel and LED drivers were controlled by computer using LabView software. Two sets of filters were used, one for fluorescence detection (RG610 and BP635 ± 5 nm, Schott) and one for phosphorescence detection (RG 695). Excitation was performed using 408 nm radiation from a cluster of 6 LEDs generating a homogeneous fluence rate of 5 mW cm^{-2} at the side of the cuvette. A dark current image was taken before and after each image and the average subtracted.

#4089 - $15.00 US Received 25 March 2004; revised 9 April 2004; accepted 15 April 2004

3. Results

The measured phosphorescence/fluorescence ratio as a function of pO_2 during illumination is shown in Fig. 2. The range of pO_2 values was realised by measuring at different distances from the air-liquid interface in a thin (1x10x25-mm) cuvette imaged from the side. The oxygen sensor needle was moved in 100μm steps, and the Phosphorescence/fluorescence ratio determined just in front of needle.

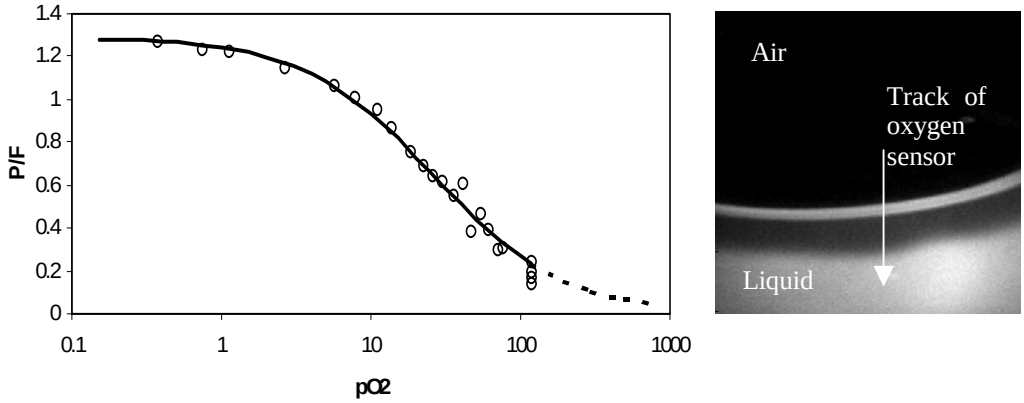

Fig. 2. Phosphorescence/fluorescence ratio as a function of the pO_2 (left). Measurements were made in a cuvette using a 100 μm sensor needle positioned at different distances from the air-liquid interface (see ratio image on right). The curve is the best fit of eq.4 with a critical pO_2 of 26 mm Hg (see discussion).

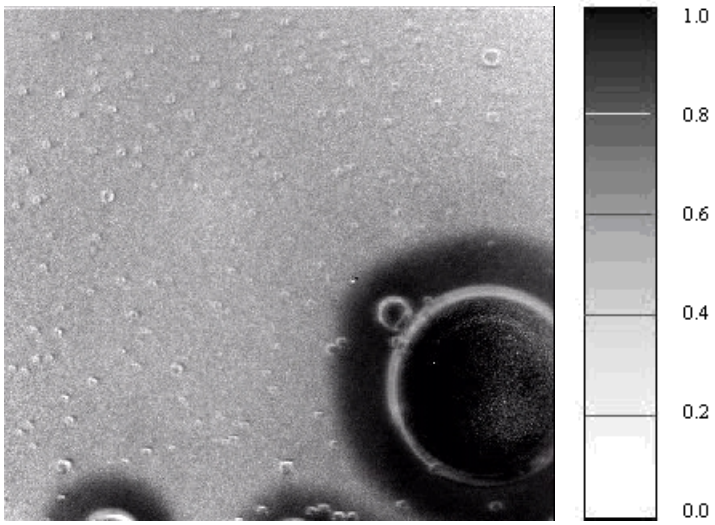

Fig. 3. (2.74 MB) Movie (100 frames, 25 seconds per frame) of the phosphorescence fluorescence ratio during PDT in a thin cuvette with a few airbubbles. The dark areas represent high oxygen levels, while the grey areas with increased phosphorescence indicate a decrease in oxygen levels. The bar refers to the value of α (eq.4); The total width of the image is 4.7 mm (size 1.28 Mb).

Figure 3 shows a sequence of images acquired from the bottom of the cuvette at 25 second intervals. In the upper left half of the image the pO_2 level has dropped within the acquisition time of the first image (25 s) to a value low enough to induce substantial phosphorescence emission. Initially in the circular areas around the two small bubbles in the lower centre and left of the image the phosphorescence emission is lower because of oxygen diffusion from

#4089 - $15.00 US Received 25 March 2004; revised 9 April 2004; accepted 15 April 2004

within each bubble. As the illumination progresses phosphorescence in this region gradually increases, as oxygen is depleted within each bubble. Around the larger bubble on the lower right the dark zone decreases in size, but does not disappear completely during the 2500 seconds of the experiment.

4. Discussion and conclusion

The effectiveness of PDT is determined by the generation of sufficient cumulative amount of singlet oxygen throughout the treatment volume. This depends not only on sensitiser concentration and light fluence, but also on both the tissue vasculature and the oxygen diffusion distance; i.e., the action radius of PDT. As described by Foster *et al*. [19] this diffusion distance is an important parameter for PDT. The sequence of images in figure 3 illustrates the PDT action radius. It shows the (dark) areas where the depletion of oxygen by consumption is compensated by diffusion from areas of high pO_2. A similar situation occurs during PDT *in vivo*: i.e. an oxygen rich environment close to blood vessels and oxygen levels too low for effective PDT at more distant locations. The size of the PDT action radius depends on the vascular pO_2, the diffusion coefficient, fluence rate and the sensitiser concentration. The phenomena observed in this study closely follow the mathematical model presented by Foster et al. [19] who describe a direct relation between the size of the oxygenated zone and the pO_2 inside a bloodvessel during PDT. If we assume an initial bubble pO_2 of 120 mmHg we calculate that from the size of the bubble and the dark zone around an initial SnMP-PDT oxygen consumption rate of 12 μM/sec. This is of the same order of magnitude as found by Foster *et al*. who calculated 6 μM/sec for protoporphyrin IX.

In theoretical analysis for the in-vitro study presented, we have not considered the influence of tissue optical properties on the measured signals of fluorescence and phosphorescence that may occur when the technique is applied in-vivo. A positive side effect of the ratioing approach is that it compensates for the photobleaching of the photosensitiser during PDT. In addition, it cancels out the excitation fluence rate Φ from the equations and hence spatial variations in the excitation intensity or the absorption and scattering properties of the tissue at this wavelength will not influence the ratio image. A complicating factor *in-vivo* is that the spectral separation between fluorescence and phosphorescence required to enable this measurement makes it unlikely that the escape functions at the phosphorescence and fluorescence wavelengths are identical. Hence, this part of the equation does not cancel out in the ratioing procedure. The importance of this effect will be dependent on the difference in emission wavelengths of phosphorescence and fluorescence and will be dependent on the particular photosensitiser used .

The study presented here was performed with SnMP, a commercially available photosensitiser that combines a high phosphorescence quantum yield with good spectral separation between fluorescence and phosphorescence. This is not a common feature of photosensitisers, in fact, only very few photosensitisers phosphoresce. These in vitro experiments have shown the feasibility of using the ratio of phosphorescence and fluorescence for treatment monitorring and we hope that it can encourage developers of new photosensitising agents to include the phosphorescent and fluorescent properties of the drugs in their evaluation. In fact, it is common practice to judge the suitability of a photosensitiser for PDT by properties like the absorption coefficient and the triplet quantum yield. The present study, however, indicates that for the evaluation of new photosensitisers the critical pO_2, i.e the oxygen level at which the triplet quenching rate is matched by the spontaneous decay rate:

$$\left[{}^3O_2\right]_{crit} = \frac{A_{20} + k_{20}}{q} \tag{7}$$

is important parameter to predict its possible clinical effectiveness.

#4089 - $15.00 US Received 25 March 2004; revised 9 April 2004; accepted 15 April 2004